TAILORING LINEAR MODELS FOR JOINT REPRESENTATION

Anonymous authors
Paper under double-blind review

ABSTRACT

The need to represent a long data series using a sequence of line segments abiding by a maximum error threshold arises in various domains. This problem, known as *Piecewise Linear Approximation* (PLA), has a long history and has recently gained attention with the rise of applications dealing with time-stamped data. State-of-the-art PLA methods achieve space savings over *lossless compression* techniques with tolerable precision loss by quantizing starting points and representing similar line segments jointly. However, these methods *do not* tailor line segments for their eventual joint representation and do not minimize the number of segments either. In this paper, we present TAILORPIECE, a suite of algorithms for lossy PLA-based compression that explicitly tailor linear segments for both small sequence length and joint representation under a given error threshold and starting-value quantization. Our first algorithm, TAILORPIECEDP, optimizes a *mergeability* criterion of PLA segment descriptions; in a degenerate form, it reduces to an algorithm that represents the data series by the minimum number of PLA segments. Our second algorithm, TAILORPIECEGD, greedily selects the endpoint of each PLA segment within a tunable search space that allows the subsequent segment to extend farther, thereby balancing compression and runtime. Through experimentation, we show that TAILORPIECEDP achieves improvements of up to 34% over prior art in compression ratio and TAILORPIECEGD gains similar savings with a runtime reduced by two orders of magnitude.

1 INTRODUCTION

Sectors like healthcare, food supply, and transportation increasingly rely on high-frequency time-series data from diverse sources (Botta et al., 2016; Xu et al., 2014; Atzori et al., 2010), to support automation, monitoring, and other advances (Gupta et al., 2020). Yet the sheer data volume renders storage costly (Jensen et al., 2018). Various encodings advance *lossless* floating-point compression (Liakos et al., 2022; 2024; Kuschewski et al., 2023; Afroozeh et al., 2023), offering gains over the widely used lossless compression algorithm, Gorilla (Pelkonen et al., 2015). Still, even these representations usually attain a compression ratio below 2, hence remain costly (Chen et al., 2024).

Lossy compression offers an alternative to lossless methods for storing large time-series datasets, allowing control of space requirements via a tunable *maximum error threshold*. Modern Time-Series Management Systems (TSMS) (Jensen et al., 2018; 2019) let users find the shortest Piecewise Linear Approximation (PLA) sequence that approximates a time-series within a desired maximum error threshold (Elmeleegy et al., 2009; Hakimi & Schmeichel, 1991) to meet their compression needs. The L_∞ norm target is often preferred to L_1 or L_2, as it bounds the error for each data record rather than just in aggregate (Karras & Mamoulis, 2008; Luo et al., 2015). A recent proposal, MIXPIECE (Kitsios et al., 2024), compresses time-series with maximum error guarantees by quantizing PLA segment starting values by the given error threshold and *jointly* representing segments having common starting values and overlapping allowable *slopes*, yielding extra space savings as Figure 1 shows. However, MIXPIECE does not ensure minimum sequence length (i.e., number of segments) nor configures segments for joint representation. Methods

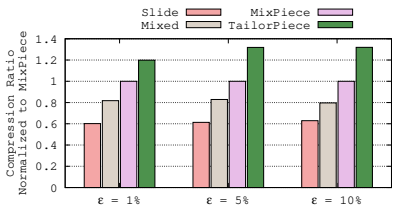

Figure 1: TAILORPIECE enhances PLA sequence length and mergeability.

that minimize sequence length under an error bound (Elmeleegy et al., 2009; Hakimi & Schmeichel, 1991) disregard *quantized* starting values and are therefore inapplicable.

In this paper, we propose TAILORPIECE, a suite of algorithms that tailor PLA segments aiming at small sequence length and joint representation:

- MINSEGMENTS, a dynamic programming algorithm that returns a *minimum-length* PLA representation with quantized starting values under a maximum error threshold.
- TAILORPIECEDP, which, building on top of TAILORPIECEDP, produces segments with wide permissible slope intervals to enhance their mergeability, and merges them.
- TAILORPIECEGD, a greedy algorithm that selects each segment's end to maximize the *next* segment's reach and allows tuning its endpoint search space to trade runtime for compression.

Our algorithms unlock the potential of grouping short PLA sequences, improving the average compression ratio by up to 34% over MIXPIECE, as Figure 1 shows. Remarkably, TAILORPIECEGD achieves slightly larger space savings than MINSEGMENTS, as it produces PLA segments more likely to be grouped, while being two orders of magnitude faster.

2 BACKGROUND

PLA with maximum error guarantees PLA represents a series of timestamped values $\langle t_i, v_i \rangle_{i \geq 1}$ by *line segments*. Some PLA methods *join* consecutive segments at their *knots* (Elmeleegy et al., 2009; Gritzali & Papakonstantinou, 1983; Hakimi & Schmeichel, 1991), others assume *disjoint* knots (Stone, 1961; Pavlidis, 1973; O'Rourke, 1981; Elmeleegy et al., 2009), and some consider both (Luo et al., 2015). We consider *disjoint* knots, where each segment may be non-continuous with its predecessor. We describe each segment by its start timestamp t_i, value v_i, and slope a_i. Common norms are L_2 (Euclidean distance) and L_∞ (maximum absolute error). We focus on L_∞, to keep *each* value within error ϵ. SLIDE (Elmeleegy et al., 2009; O'Rourke, 1981) finds the *minimum-length* disjoint PLA sequence under a maximum error threshold, greedily building the convex hull of data points in the segment under construction to maintain the admissible slope range.

MIXPIECE (Kitsios et al., 2024), the leading PLA method, *quantizes* segment starting values and *jointly* represents segments with common starting values and overlapping admissible *slope intervals* with a *minimum* number of groups by partitioning an *interval graph*, whose edges denote overlapping intervals, into the fewest *cliques* (Kitsios et al., 2023) in $O(n \log n)$ time (Gupta et al., 1982).

3 OVERVIEW

We aim to reduce the storage requirements of PLA representations under a maximum-error threshold ϵ. While the MIXPIECE (Kitsios et al., 2024) storage model merges segment descriptions to minimize the *number of groups* given a set of segments, it does *not* minimize the number of PLA segments given a starting-value quantization and error threshold ϵ. We first address this open problem with a dynamic programming algorithm, MINSEGMENTS, that *provably* returns the *shortest* PLA sequence for the same quantization and error threshold. With MINSEGMENTS as a foundation, we propose TAILORPIECEDP, which enhances the mergeability of linear segments to attain further space savings. Lastly, we propose TAILORPIECEGD, a greedy algorithm that attains space savings similar to MINSEGMENTS at two orders of magnitude lower execution time.

3.1 QUANTIZED REACH

As a preparatory step, we extract Procedure 3.1 from MIXPIECE (Kitsios et al., 2024), which selects the longest among the linear segments starting from each original value v, ϵ-*quantized* to the nearest lower b^- or higher b^+ multiple of ϵ:

$$\begin{aligned} b^- &= \lfloor v/\epsilon \rfloor \times \epsilon \\ b^+ &= \lceil v/\epsilon \rceil \times \epsilon \end{aligned} \tag{1}$$

Procedure 3.1: ϵ-quantized reach(s, i, ϵ)

input : Starting index i, data signal s: $\langle t_i, v_i\rangle\ \forall i \in \{1, \ldots, n\}$, error threshold ϵ
output : ϵ-quantized reach of i

1 $reach \leftarrow 0$; s.seek(i); $\langle t_s, v_s\rangle \leftarrow s$.next();
// quantize v_s to the nearest lower (b^-) and higher (b^+) multiples of ϵ
2 $b^- \leftarrow \lfloor v_s/\epsilon \rfloor \epsilon$; $b^+ \leftarrow \lceil v_s/\epsilon \rceil \epsilon$;
3 $a_{u^-} \leftarrow \infty$; $a_{l^-} \leftarrow -\infty$; $a_{u^+} \leftarrow \infty$; $a_{l^+} \leftarrow -\infty$;
4 $floor \leftarrow true$; $ceil \leftarrow true$;
5 **while** *s.hasNext()* **do**
6 $\langle t_c, v_c\rangle \leftarrow s$.next();
7 **if** $v_c > a_{u^-}(t_c - t_s) + b^- + \epsilon$ ***or*** $v_c < a_{l^-}(t_c - t_s) + b^- - \epsilon$ **then**
8 $floor \leftarrow false$; // stop b^- segment
9 **if** $v_c > a_{u^+}(t_c - t_s) + b^+ + \epsilon$ ***or*** $v_c < a_{l^+}(t_c - t_s) + b^+ - \epsilon$ **then**
10 $ceil \leftarrow false$; // stop b^+ segment
11 **if** $floor$ ***or*** $ceil$ **then** $reach++$; // within bounds
12 **else return** $reach$; // out of bounds
13 **if** $v_c < a_{u^-}(t_c - t_s) + b^- - \epsilon$ **then** $a_{u^-} \leftarrow \frac{v_c+\epsilon-b^-}{t_c-t_s}$; // lower slope
14 **if** $v_c > a_{l^-}(t_c - t_s) + b^- + \epsilon$ **then** $a_{l^-} \leftarrow \frac{v_c-\epsilon-b^-}{t_c-t_s}$; // raise slope
15 **if** $v_c < a_{u^+}(t_c - t_s) + b^+ - \epsilon$ **then** $a_{u^+} \leftarrow \frac{v_c+\epsilon-b^+}{t_c-t_s}$; // lower slope
16 **if** $v_c > a_{l^+}(t_c - t_s) + b^+ + \epsilon$ **then** $a_{l^+} \leftarrow \frac{v_c-\epsilon-b^+}{t_c-t_s}$; // raise slope
17 **return** $reach$;

For instance, with $\epsilon = 0.5$, each of values 1.1 and 1.4 yields $b^- = 1$ and $b^+ = 1.5$. Figure 2 illustrates the process. Two angles, one initiated from $\langle t_1, b^-\rangle$ (Figure 2a) with bounding slopes $a^-_{u_2}$ and $a^-_{l_2}$ (Line 13–Line 14) and one from $\langle t_1, b^+\rangle$ (Figure 2b) with bounding slopes $a^+_{u_2}$ and $a^+_{l_2}$ (Line 15–Line 16), both subtended by $\langle t_2, v_2 + \epsilon\rangle$ and $\langle t_2, v_2 - \epsilon\rangle$, enclose all lines starting from b^- or b^+ that approximate the two seen points within ϵ. As the next point, $\langle t_3, v_3\rangle$, lies within both angles, yet more than ϵ away from their upper and lower slopes, we reduce them to $(a^-_{u_3}, a^-_{l_3})$ (Figure 2a) and $(a^+_{u_3}, a^+_{l_3})$ (Figure 2b), subtended by $\langle t_3, v_3 + \epsilon\rangle$ and $\langle t_3, v_3 - \epsilon\rangle$. Next, point $\langle t_4, v_4\rangle$ lies outside the angle formed by $(a^-_{u_3}, a^-_{l_3})$ (Figure 2a), hence cannot be approximated by a segment starting at b^- (Line 10). Contrariwise, a further reduction of the angle starting from b^+ approximates point $\langle t_4, v_4\rangle$ with ϵ, we thus set its upper slope to $a^+_{u_4}$, connecting $\langle t_1, b^+\rangle$ to $\langle t_4, v_4 + \epsilon\rangle$ and retain the lower slope $a^+_{l_3}$, already within ϵ of $\langle t_4, v_4\rangle$. The gray area in Figure 2b captures the candidate lines within ϵ of all four points.

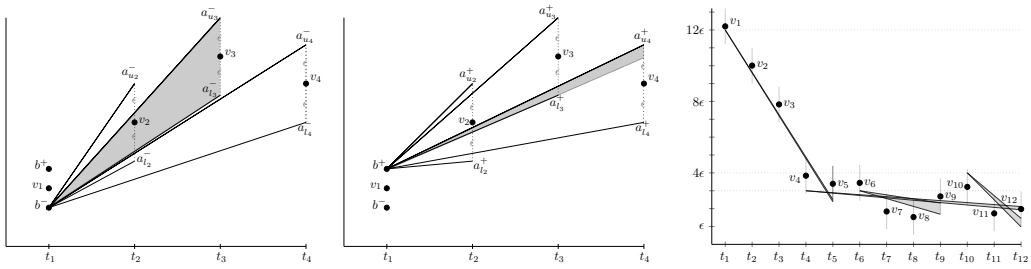

(a) Angle with b^- as origin. (b) Angle with b^+ as origin. (c) Using best of b^- and b^+ wrt r_i.

Figure 2: MIXPIECE opts for the segment starting from b^+ (Figure 2b) and reaching t_4 over that starting from b^- (Figure 2a) reaching t_3. Figure 2c shows the longest segments from t_1, t_4, t_6, t_{10}.

We establish the correctness of Procedure 3.1 as follows.

Definition 1 *The* ϵ-quantized reach r_i *of timestamp* t_i *in a signal* $s = \langle t_i, v_i\rangle$, $i \in \{1, \ldots, n\}$, *is the* maximum *length of a linear segment that starts from an* ϵ*-quantization of* v_i *and approximates subsequent values in* s *within* ϵ.

Procedure 3.1 returns the *ϵ-quantized reach* of i.

Without loss of generality, assume Procedure 3.1 returns r_i for point $\langle v_1, t_1\rangle$, while there exists a linear segment of length $r_i + 1$ that starts from a quantization of v_1 and is within ϵ from all points up to $\langle t_{i+1}, v_{i+1}\rangle$. This line necessarily belongs to the set computed by Procedure 3.1 up to point $\langle t_i, v_i\rangle$. Then the procedure should not have stopped at timestamp t_i, a contradiction. Thus, Procedure 3.1 returns the maximum length.

We configure our implementation of Procedure 3.1 to return the *bounding slopes* of the longest segment, in addition to its length.

3.2 MINIMIZING THE NUMBER OF SEGMENTS

The greedy strategy of Procedure 3.1, used in (Kitsios et al., 2024), maximizes *reach* from a given point but ignores global optimality. On the signal of Figure 2c, it selects segment $[t_1, t_5]$, then $[t_6, t_9]$, and $[t_{10}, t_{12}]$.

Yet, as Figure 3 shows, reach r_4 spans farther than r_6 and r_{10} combined, so two segments—$[t_1, t_3]$ and $[t_4, t_{12}]$—suffice to approximate the signal. This counterintuitive outcome arises because r_i, being dependent on the quantization of v_i to either b_i^- or b_i^+, exceeds $\delta i + r_{i+\delta i}$, hence starting at i is preferable to starting at $i + \delta i$. The greedy algorithm is thus suboptimal. We define the problem of finding a minimum-length PLA under quantization as follows:

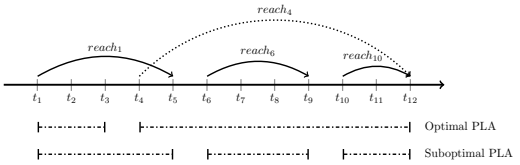

Figure 3: Maximally extending each segment may lead to a suboptimal sequence length: r_4 surpasses $r_6 + r_{10}$, hence we reach t_{12} with two segments by ending the first segment at t_3.

Problem 1 *Given data sequence s:* $(t_i, v_i), i \in \{1, \ldots, n\}$ *and error threshold* ϵ*, find a minimum-length PLA sequence of disjoint segments from* ϵ-quantized *values, to approximate* s *within* ϵ*.*

Algorithm 3.2 lists MINSEGMENTS, a dynamic-programming solution to Problem 1 that gets each starting point's *reach*(Line 3) via Procedure 3.1 and recursively derives the least PLA length from t_i (Line 8):

$$L(i) = \begin{cases} \min_{i<j\leq i+r_i}\{L(j+1)+1\}, & i < n \\ 1, & i = n \\ 0, & i > n \end{cases} \quad (2)$$

Algorithm 3.2: MINSEGMENTS (s, ϵ)

```
input  : Signal s: (t_i, v_i) ∀i ∈ {1,...,n}, error threshold ε
output : A minimum-length PLA sequence on s
1  i ← 1;
2  while s.hasNext() do
3      r[i] ← ε_quantized_reach(s, i, ε);
4      s.next();
5      i++;
6  i ← N;
7  while i ≥ 1 do
8      Compute L[i]; // by Equation (2)
9      i − −;
10 return L[1];
```

Figure 4 depicts MINSEGMENTS's computation for the signal of Figure 2c. The left side shows the *reach* of starting points, while the right side computes the optimal PLA sequence length starting from each point via Equation (2). Since $r_1 = 4$, the first segment may end at any of $\langle t_2, t_3, t_4, t_5 \rangle$. With $L(2)$, $L(3)$, and $L(5)$ larger than 1, and $L(4) = 1$, we end the first segment at t_3 and approximate the signal using only *two* segments, exploiting the large reach r_4. MINSEGMENTS (Algorithm 3.2) returns a globally optimal solution to Problem 1 via the recursive minimization in Equation (2) in $O(Rn)$ time, where R is the maximum reach in the signal, as each recursion step is linear in r_i for each i. For small maximum error thresholds, R is typically a small constant. Our implementation of Algorithm 3.2 also returns the starting points and *bounding slopes* (as in Section 3.1) of segments in the minimum-length PLA sequence, along with the sequence length.

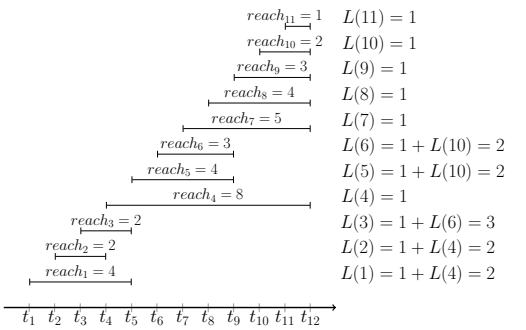

Figure 4: Computing least PLA sequence length.

3.3 TAILORPIECEDP ALGORITHM

Each segment in the PLA of Algorithm 3.2 has two *bounding slopes* defining its admissible slope range for line segments that approximate the data therein. We define *slope interval size* as follows.

Definition 2 *The* slope interval size I_k *of segment* k^{th} *is the gap between its upper and lower slopes.*

In Figure 2a, $I_1 = a_{u_3}^- - a_{l_3}^-$, and in Figure 2b, $I_1 = a_{u_4}^+ - a_{l_3}^+$.

By MIXPIECE's storage model, we aim to merge and jointly represent segments with coinciding starting points and overlapping slope intervals. However, Equation (2) may miss the best compression: it shortens the PLA sequence yet overlooks the slope interval sizes of the segments it creates. *Larger* intervals are preferable, as they are more likely to overlap. Accordingly, we enhance MINSEGMENTS to TAILORPIECEDP, which yields segments with larger slope intervals to boost overlap among them and enable further segment grouping. To craft TAILORPIECEDP, we refine TAILORPIECEDP's objective to a composite function $C(i)$ that favors both large slope intervals and few segments starting at timestamp $t_i, i \geq 1$. The average slope interval size over $L(i)$ segments is $\frac{\sum_{k=1}^{L(i)} I_k}{L(i)}$. To modulate the influence of individual slope interval sizes, we introduce an

exponent $p \in [0, 1]$ on the numerator terms, yielding $\frac{\sum_{k=1}^{L(i)} {I_k}^p}{L(i)}$. To ease the recursion, we define the numerator aggregate as $S(i) = \sum_{k=1}^{L(i)} {I_k}^p$. For $p = 0$, the fraction equals 1, as the number of segments divided by itself. For $p > 0$, it favors many short segments that yield large slope intervals. To counter this effect and favor fewer segments, we additionally normalize by $L(i)$, yielding a squared denominator in our composite objective: $C(i) = \frac{S(i)}{L(i)^2}$.

Problem 2 *Given a data sequence s: $(t_i, v_i), i \in \{1, \ldots, n\}$, and a maximum absolute error threshold ϵ, find a PLA sequence of disjoint linear segments, each starting from an ϵ-*quantized *value, that approximates s within ϵ and maximizes $C(i) = \frac{S(i)}{L(i)^2}$.*

Equation (3) solves Problem 2 by recursively maximizing $C(i)$; $I(i, j)$ denotes the slope interval size of the segment from t_i to t_j, while $S(i)$ and $L(i)$ assume the values of the optimizing numerator and denominator, respectively, in each recursion step.

$$C(i) = \begin{cases} \max_{i<j\leq i+r_i} \left\{ \frac{S(j+1)+I(i,j)^p}{(L(j+1)+1)^2} \right\} & i < n \\ 1 & i = n \\ 0 & i > n \end{cases} \tag{3}$$

TAILORPIECEDP replaces $L[i]$ with $\{C[i], S[i], L[i]\}$ in Lines 8 and 10 and returns $C[1]$ in place of $L[1]$ in Line 10 of Algorithm 3.2. Exponent p enables fine-grained control and links TAILORPIECEDP to MINSEGMENTS: $p = 0$ reduces TAILORPIECEDP to minimizing segments, as MINSEGMENTS does. In our experiments, TAILORPIECEDP with a broad range of p values outperform MINSEGMENTS across datasets.

3.4 TAILORPIECEGD ALGORITHM

TAILORPIECEDP seeks a PLA sequence that approximates a signal within a threshold ϵ using segments with ϵ-quantized starting values and maximizes $C(i) = \frac{S(i)}{L(i)^2}$. However, optimality comes at the cost of higher computational overhead.

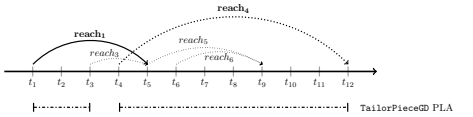

Figure 5: TAILORPIECEGD ends the first segment at t_3 to reach t_{12} with two segments.

Here, we propose TAILORPIECEGD, a greedy algorithm that offers an attractive tradeoff between the efficiency of MIXPIECE (Kitsios et al., 2024) and the effectiveness of TAILORPIECEDP. Its core idea is to reduce the myopic behavior of MIXPIECE by enhancing lookahead when forming a segment. Figure 5 illustrates an example where a segment starting at t_1 may reach t_5. MIXPIECE would create this segment and begin the next one at t_6. However, we may instead end the first segment earlier—at t_2, t_3 or t_4—and start the next segment at the following point. Among these alternatives, ending the first segment at t_3 leads to the best outcome, as the long reach of r_4 allows the next segment to extend to t_{12}, whereas segments starting after t_2, t_4, or t_5, may only reach up to t_9. TAILORPIECEGD, outlined in Algorithm 3.3, considers several candidate endpoints j (beyond the default $i + r_i$ used by MIXPIECE) for the segment starting at i. For each j, it evaluates the reach of the next segments starting at $j + 1$, and selects the *earliest* point $j_{\min}$ among those that yield the largest combined reach of the two segments. Choosing the *earliest* qualifying endpoint promotes larger slope intervals, as the breadth of a slope interval is a non-increasing function of segment length, and thereby enables more effective groupings. This exhaustive examination of end-

Algorithm 3.3: TAILORPIECEGD (s, ϵ)

Input: Data signal s: $\langle t_i, v_i \rangle \ \forall i \in \{1, \ldots, n\}$, error threshold ϵ
Output: Array $b\_intervals$ mapping each quantized value to $\langle a_l\ a_u\ t \rangle$ tuple list
Function TAILORPIECEGD (s, ϵ)
$b\_intervals \leftarrow \{\{\}, \ldots, \{\}\}$; $\langle t_s, v_s \rangle \leftarrow s$.next();
$b^- \leftarrow \lfloor v_s/\epsilon \rfloor \epsilon$; $b^+ \leftarrow \lceil v_s/\epsilon \rceil \epsilon$; // quantized starting points
$a_{u^-} \leftarrow \infty$; $a_{l^-} \leftarrow -\infty$; $a_{u^+} \leftarrow \infty$; $a_{l^+} \leftarrow -\infty$; // slope intervals
$floor \leftarrow true$; $ceil \leftarrow true$; $diff \leftarrow 0$; $i \leftarrow 1$;
$j_{\min} \leftarrow \min\{\arg\max_{j \in [i+r_i^q, i+r_i]} \{j + r_{j+1}\}\}$; // Equation (4)
while *s.hasNext()* **do**
  $\langle t_c, v_c \rangle \leftarrow s$.next();
  $i++$;
  if $v_c > a_{u^-}(t_c - t_s) + b^- + \epsilon$ ***or*** $v_c < a_{l^-}(t_c - t_s) + b^- - \epsilon$ **then**
    $floor \leftarrow false$;
  if $v_c > a_{u^+}(t_c - t_s) + b^+ + \epsilon$ ***or*** $v_c < a_{l^+}(t_c - t_s) + b^+ - \epsilon$ **then**
    $ceil \leftarrow false$;
  if $floor$ **then** $diff++$;
  if $ceil$ **then** $diff--$;
  if $i > j_{min}$ **then** // close segment when reaching j_{min}
    if $diff > 0$ **then** $b\_intervals[b^-]$.add($\langle a_{l^-}, a_{u^-}, t_s \rangle$);
    else $b\_intervals[b^+]$.add($\langle a_{l^+}, a_{u^+}, t_s \rangle$);
    $\langle t_s, v_s \rangle \leftarrow \langle t_c, v_c \rangle$;
    $b^- \leftarrow \lfloor v_s/\epsilon \rfloor \epsilon$; $b^+ \leftarrow \lceil v_s/\epsilon \rceil \epsilon$;
    $a_{u^-} \leftarrow \infty$; $a_{l^-} \leftarrow -\infty$; $a_{u^+} \leftarrow \infty$; $a_{l^+} \leftarrow -\infty$;
    $floor \leftarrow true$; $ceil \leftarrow true$; $diff \leftarrow 0$;
    $j_{\min} \leftarrow \arg\max_{j \in [i+r_i^q, i+r_i]} \{j + r_{j+1}\}$; // Equation (4)
  if $v_c < a_{u^-}(t_c - t_s) + b^- - \epsilon$ **then** // lower slope
    $a_{u^-} \leftarrow \frac{v_c + \epsilon - b^-}{t_c - t_s}$;
  if $v_c > a_{l^-}(t_c - t_s) + b^- + \epsilon$ **then** // raise slope
    $a_{l^-} \leftarrow \frac{v_c - \epsilon - b^-}{t_c - t_s}$;
  if $v_c < a_{u^+}(t_c - t_s) + b^+ - \epsilon$ **then** // lower slope
    $a_{u^+} \leftarrow \frac{v_c + \epsilon - b^+}{t_c - t_s}$;
  if $v_c > a_{l^+}(t_c - t_s) + b^+ + \epsilon$ **then** // raise slope
    $a_{l^+} \leftarrow \frac{v_c - \epsilon - b^+}{t_c - t_s}$;
if $diff > 0$ **then** $b\_intervals[b^-]$.add($\langle a_{l^-}, a_{u^-}, t_s \rangle$);
else $b\_intervals[b^+]$.add($\langle a_{l^+}, a_{u^+}, t_s \rangle$);
return $b\_intervals$;

points reduces PLA sequence length and increases slope interval breadth, yet it also incurs a runtime overhead. To manage this cost, we restrict the set of candidate endpoints for each segment using an exponent parameter $q \in [0, 1]$:

$$j_{\min} = \min \left\{ \underset{j \in [i+r_i^q, i+r_i]}{\arg\max} \left\{ j + r_{j+1} \right\} \right\} \tag{4}$$

The r_i^q term in Equation (4) sets the minimum segment length. For $q = 0$, Equation (4) checks all eligible endpoints j, and, as our experiments show, gains space savings on par with or better than those of MINSEGMENTS. The growth of q drops candidate endpoints near the segment's start. Intuitively, segments that underuse a starting point's reach are unlikely to serve in the shortest PLA sequence. By contrast, q near 1 curbs both search space and compression. At $q = 1$, TAILORPIECEGD reduces to MIXPIECE, considering only the endpoint $i + r_i$ for a segment starting at i.

4 EXPERIMENTAL RESULTS

We ran experiments on a 3.3GHz Intel® Core™i5-4590 machine with 6MB L3 cache and 16GB DDR3 1.6GHz RAM. We implemented[1] our algorithms in Java and compared performance against:

- Methods for the L_∞ error metric:
  - SLIDE[2] (Elmeleegy et al., 2009), which optimally solves *disjoint PLA* using a convex hull.
  - MIXED [2] (Luo et al., 2015), which finds a least-length PLA of *mixed joint and disjoint* segments.
  - MIXPIECE[3] (Kitsios et al., 2024), the leading method for jointly representing PLA segments.
- Methods designed for the L_2 error metric:
  - Bottom-Up[4] (Keogh et al., 2001b), which merges in turn adjacent segments yielding least error.
  - PAA (Keogh et al., 2001a), which represent equi-sized segments, each with the mean of its values.
  - DFT (Cooley & Tukey, 1965), which uses the first few Discrete Fourier Transform features.
  - HIRE[5] (Barbarioli et al., 2023), which constructs a synopsis data structure through a recursion of partitioning, piecewise approximation, and residualization steps at increasingly finer granularity.
- Camel[6] (Yao et al., 2024), which separately compresses the integer and decimal parts of double-precision floating-point numbers, to a precision of four decimal places.

We evaluate solutions on all datasets of the UCR Time Series Classification Archive[7] that do not contain undefined values. Given that *lossless* algorithms (Yao et al., 2024) achieve compression ratios up to 4, we relegated data that cannot be compressed by a ratio of at least 10 with $\epsilon = 1\%$ as unsuitable for PLA-based compression. Used SLIDE (Elmeleegy et al., 2009) to ensure fairness, we compressed all data with a maximum error at 1% of the signal's range and selected those that attained compression greater than 10, ending up with 41 datasets, which we use in our experiments. For completeness, we also report aggregate results for the entire archive.

4.1 PLA SEQUENCE LENGTH

We commence by assessing the length of produced PLA sequences. Table 1 reports the number of segments MIXPIECE, MINSEGMENTS, TAILORPIECEGD and TAILORPIECEDP furnish, expressed as a percentage over the minimum achievable disjoint PLA sequence length under a maximum error threshold (Luo et al., 2015), obtained using SLIDE (Elmeleegy et al., 2009; O'Rourke, 1981), for ten maximum error values in $[1\%, 10\%]$ of the signal's range.

[1] https://anonymous.4open.science/r/pla-compression
[2] https://cse.hkust.edu.hk/~yike/PLAcode.rar
[3] https://github.com/xkitsios/Mix-Piece_Sim-Piece
[4] https://github.com/NickFoubert/simple-segment
[5] https://github.com/gmersy/HIRE
[6] https://github.com/yoyo185644/camel
[7] https://www.cs.ucr.edu/~eamonn/time_series_data/

Table 1 shows that MIXPIECE produces PLA sequences $7.5\% - -9.3\%$ longer than the minimum, leaving room for improvement. MINSEGMENTS cuts this to $5.3\% - -7.4\%$, minimizing disjoint segments with $\epsilon-$quantized starting points, which favor grouping, while SLIDE selects starting points freely, thus produces shorter PLA sequences. TAILORPIECEGD performs even better: despite its greedy strategy, it adds only 0.1–0.2% segments over MINSEGMENTS for $\epsilon = 1\% - -10\%$, yielding PLA lengths close to the optimum. TAILORPIECEDP produces the same segments as MINSEGMENTS for small p (e.g., 2^{-20}). Section 4.6 discusses the effect of p on TAILORPIECEDP in more detail.

Table 1: Extra segments over the least floating-starting-value disjoint segments by SLIDE.

ϵ	Slide (segments)	MIXPIECE	MINSEGMENTS	TAILORPIECEGD ($q = 0$)	TAILORPIECEDP ($p = 2^{-20}$)
1%	2786.0	+9.3%	+6.6%	+6.7%	+6.6%
2%	1805.6	+7.9%	+5.3%	+5.4%	+5.3%
3%	1419.0	+7.9%	+5.5%	+5.6%	+5.5%
4%	1209.3	+7.5%	+5.5%	+5.6%	+5.5%
5%	1051.1	+8.3%	+6.0%	+6.1%	+6.0%
6%	939.7	+8.2%	+6.1%	+6.2%	+6.1%
7%	839.2	+8.9%	+6.7%	+6.8%	+6.7%
8%	758.4	+8.4%	+6.6%	+6.7%	+6.6%
9%	696.9	+9.1%	+7.4%	+7.5%	+7.4%
10%	646.3	+8.8%	+7.0%	+7.2%	+7.0%

4.2 COMPRESSION RATIO COMPARISON

Next, we evaluate the effectiveness of our approaches against solutions that provide maximum error guarantees, i.e., SLIDE (Elmeleegy et al., 2009), MIXED (Luo et al., 2015) and MIXPIECE (Kitsios et al., 2024). We also report results for Camel (Yao et al., 2024), without considering the overhead of timestamps, to provide a reference point with regard to the requirements of *lossless* data representation. For the sake of brevity, we exclude PMC-MR (Lazaridis & Mehrotra, 2003), and Swing (Elmeleegy et al., 2009) from this comparison, as these algorithms have been shown to underperform compared to MIXPIECE in (Kitsios et al., 2024). Lastly, we discuss the results of the Serf-XOR (Li et al., 2025) *streaming* floating-point compression algorithm, which produces very modest savings compared to the PLA approaches evaluated here.

We measure *compression ratio*, i.e., the ratio of the number of bytes in the uncompressed representation to that in the compressed one, including the representation of values and timestamps, for each method and dataset, considering that the timestamp and value of each point in the original signal require $4 + 4 = 8$ bytes.

Table 2 (in the Appendix) presents detailed results for maximum error[8] 5% and 10% of the signal's range for the 41 selected time-series, as well as averages for the remaining ones, in the UCR archive. Both MINSEGMENTS and TAILORPIECEGD improve compression ratio over MIXPIECE. On average, MINSEGMENTS provides improvements over 18% and 16% for maximum error values of 5% and 10% of the signal's range, respectively, as the myopic nature of MIXPIECE's first phase hinders joint representation. TAILORPIECEGD attains space savings commensurate to, and at times higher than, those of MINSEGMENTS, with a gain of 20% over MIXPIECE on average, as it explores a larger search space than MIXPIECE. More impressively, TAILORPIECEGD gains over MINSEGMENTS; even though TAILORPIECEGD produces more segments than MINSEGMENTS (as Table 1 documents), it yields larger slope intervals, which are more likely to allow joint representations.

Figure 6 shows the effect of using the *latest* instead of the *earliest* endpoint j among those that provide the largest combined reach for each pair of consecutive segments in TAILORPIECEGD, replacing the $\min$ with $\max$ in Equation (4). Interestingly, the use of $\max$ forfeits the advantage of TAILORPIECEGD over MINSEGMENTS, yielding segments that are less likely to be grouped. TAILORPIECEDP with a small value of p yields the best compression ratio on all datasets (including those that do not fit in Table 2), with average gains over MIXPIECE, surpassing 32% with ϵ at 5% and 10% and reaching a maximum of 34% with $\epsilon = 7\%$. Table 2 (rest, all) also shows that our solutions offer considerable improvements for the entire UCR archive, which includes datasets that are inherently harder to compress due to an unusually large variance among their neighboring values. We omit the detailed results for the

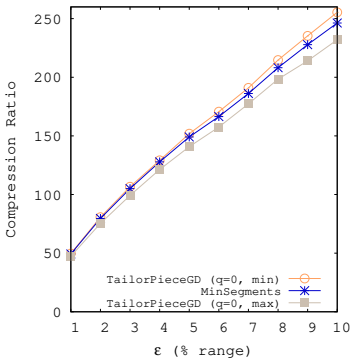

Figure 6: Using *max* instead of *min* in Equation (4) hurts performance.

[8] We omit detailed results for $\epsilon = 1\%$ due to space constraints, but present average results in Figure 11a.

Serf-XOR (Li et al., 2025)[9] streaming compression method from Table 2, as it provides very modest space savings, offering an average compression ratio of 12.08 and 13.01 for maximum error values of 5% and 10% of the signal's range, respectively, for the 41 time series in our dataset. Considering all time series, the compression ratio of Serf-XOR is 10.08 and 11.71 for $\epsilon = 5\%$ and 10%, respectively. The attained compression ratio does not improve significantly even with $\epsilon = 50\%$. As these results are non-competitive, we exclude Serf-XOR from the remainder of our experimental analysis.

4.3 Quality of Approximation

Our next experiment reports the Normalized Root Mean Squared Error (NRMSE) to assess approximation quality; we use normalized instead of plain RMSE, as value ranges vary largely across datasets. Figure 7 plots average NRMSE values vs. compression ratio, Figure 7a on the selected datasets of Table 2 and Figure 7b on the entire UCR archive. We include all algorithms that operate under a maximum error threshold and three approaches that target L_2, namely PAA (Keogh et al., 2001a), DFT (Cooley & Tukey, 1965), and Bottom-Up (Keogh et al., 2001b). For each compression ratio, algorithms with maximum error guarantees offer higher average approximation quality than those targeting L_2, such as PAA (Keogh et al., 2001a), DFT (Cooley & Tukey, 1965) and Bottom-Up (Keogh et al., 2001b). Our methods advance the state of the art, achieving lower NRMSE, hence more accurate PLA representations, than Slide, Mixed and MixPiece under the same space limits. TailorPieceGD slightly outperforms MinSegments, while TailorPieceDP attains the best quality by a wide margin. Figure 8 visualizes the segments TailorPieceDP yields for Car dataset sample at $\epsilon = 1\%$ and 5%, illustrating how segment count and approximation quality drop as ϵ rises.

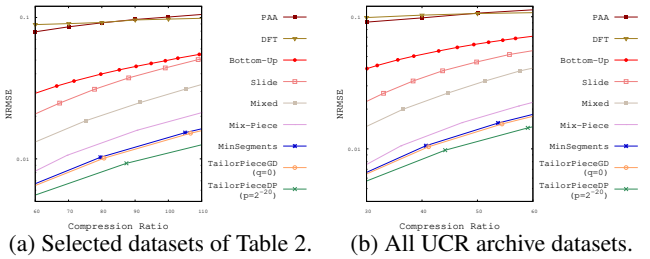

(a) Selected datasets of Table 2. (b) All UCR archive datasets.

Figure 7: NRMSE vs. compression ratio; y-axis on log scale.

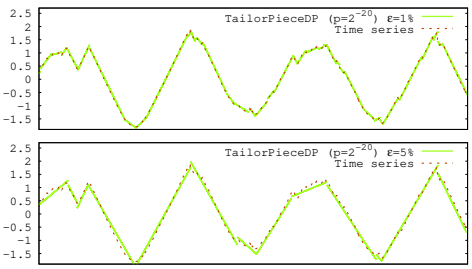

Figure 8: PLA segments, `Car` data sample.

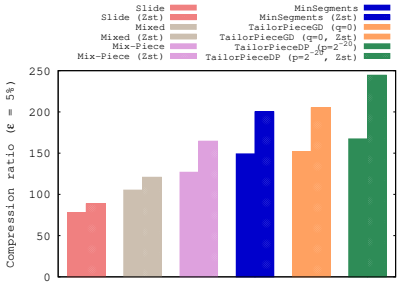

Figure 9: General compression.

4.4 General-Purpose Compression Gains

Figure 9 shows the effect of lossless general-purpose compression, Zstandard (Collet, 2015), on outputs with $\epsilon = 5\%$. Our methods yield the largest overall savings. Figure 10 shows results for L_2-targeting algorithms—PAA (Keogh et al., 2001a), DFT (Cooley & Tukey, 1965), Bottom-Up (Keogh et al., 2001b), and HIRE (Barbarioli et al., 2023)—using ZStandard, except for HIRE, which uses TRC[10]. General-purpose compression boosts the quality-space tradeoff but retains the algorithm ranking: MinSegments, TailorPieceGD, and TailorPieceDP still offer the best tradeoff. HIRE performs significantly worse.

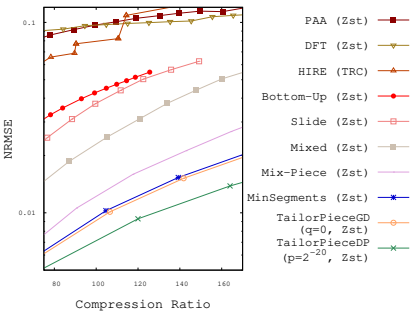

Figure 10: NMRSE with general compression on outputs; y-axis on log scale.

[9] https://github.com/Spatio-Temporal-Lab/Serf

[10] https://github.com/powturbo/Turbo-Range-Coder

4.5 COMPRESSION/TIME TRADEOFF

Figure 11 reports compression times and ratios for our algorithms and competitors. We average measurements over the datasets of Table 2 and normalize times by dataset size. TAILORPIECEGD and TAILORPIECEDP traces show performance across $q \in [0, 0.99]$ and $p \in [0, 2^{-20}]$, with MINSEGMENTS corresponding to TAILORPIECEDP at $p = 0$. Our methods outperform competitors: TAILORPIECEDP at $p = 2^{-20}$ achieves the highest space savings, improved by 20%, 32% and 32% over MIXPIECE for $\epsilon = 1\%$, 5% and 10%, respectively. TAILORPIECEGD with $q = 0$ ranks second, improving by 13%, 20% and 20% over MIXPIECE. MINSEGMENTS (i.e., TAILORPIECEDP with $p = 0$) yields slightly worse compression than TAILORPIECEGD, despite shorter PLA sequences, due to larger slope intervals that enable grouping.

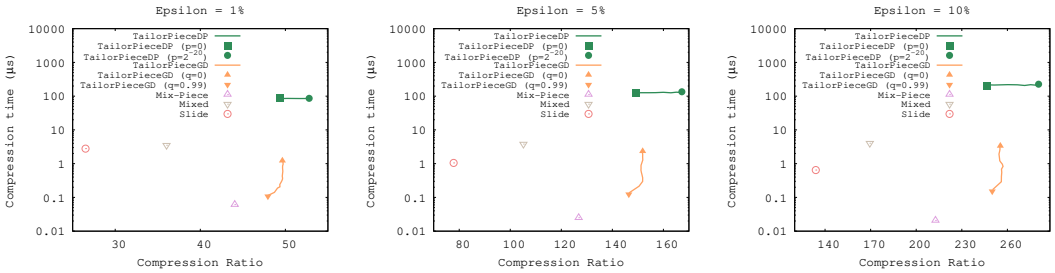

(a) (b) (c)

Figure 11: Compression time per data record vs ratio at different error thresholds.

Whereas TAILORPIECEDP incurs a notable runtime overhead, as its compression time matches that of MINSEGMENTS, making TAILORPIECEDP with small p the preferred choice when reducing space is key. TAILORPIECEGD runs two orders of magnitude faster than the dynamic-programming approaches with $q = 0$, offering an attractive tradeoff between compression ratio and execution time. As Figure 11 shows, higher q further enhances this tradeoff, with compression time on par with MIXPIECE and space savings competitive vs. $q = 0$. In effect, TAILORPIECEGD excels when compression speed matters most.

Figure 12 (in the Appendix) plots average decompression time, which is often more crucial than compression time, as data is written once but read repeatedly. Our methods surpass MIXPIECE. SLIDE and MIXED lag due to computing slope-intercept equations during decompression.

4.6 FAVORING SEGMENTS WITH LARGE INTERVALS

The dynamic-programming MINSEGMENTS algorithm minimizes PLA sequence length. However, compression also depends on slope intervals. Larger intervals increase the chance of grouping similar segments, boosting space savings, thus we favor segments with *large* slope intervals. Figure 13 (in the Appendix) illustrates the effect of exponent p of TAILORPIECEDP, which adjusts the effect of slope interval size in the objective, on the datasets of Table 2. Large p values hurt compression, as they drag TAILORPIECEDP to use more PLA segments (e.g., for $p = 2^{-1}$ and $\epsilon = 10\%$, the compression of TAILORPIECEDP is 15% worse than MINSEGMENTS). However, smaller p yields sequence length on par with MINSEGMENTS and also enlarges average interval size, as it is apparent for $p < 2^{-6}$, yielding space savings above 7%, 12% and 13.9%, for ϵ equal to 1%, 5% and 10%, respectively. The plateau beyond this point arises as p is small enough for TAILORPIECEDP to match the optimal number of segments while creating larger intervals via Equation (1).

5 CONCLUSIONS

We presented techniques to build and compress piecewise linear segments for time-series storage: MINSEGMENTS computes a minimum-length PLA with quantized starting values under a maximum error threshold. TAILORPIECEDP refines this objective to render segments more amenable to joint representation by common starting values and overlapping slope intervals, yielding extra space savings. Drawing on these insights, TAILORPIECEGD offers a tunable tradeoff between compression and runtime by limiting its greedy-search space. Experiments show TAILORPIECEGD attains space savings near MINSEGMENTS, vastly exceeding the state of the art, and runs two orders of magnitude faster and on par with existing approaches.

REFERENCES

Azim Afroozeh, Leonardo X. Kuffo, and Peter A. Boncz. ALP: adaptive lossless floating-point compression. *Proc. ACM Manag. Data*, 1(4):230:1–230:26, 2023.

Luigi Atzori, Antonio Iera, and Giacomo Morabito. The internet of things: A survey. *Computer Networks*, 54(15):2787–2805, 2010. ISSN 1389-1286. doi: https://doi.org/10.1016/j.comnet.2010.05.010. URL https://www.sciencedirect.com/science/article/pii/S1389128610001568.

Bruno Barbarioli, Gabriel Mersy, Stavros Sintos, and Sanjay Krishnan. Hierarchical residual encoding for multiresolution time series compression. *Proc. ACM Manag. Data*, 1(1):99:1–99:26, 2023.

Alessio Botta, Walter de Donato, Valerio Persico, and Antonio Pescapé. Integration of cloud computing and internet of things: A survey. *Future Generation Computer Systems*, 56:684–700, 2016. ISSN 0167-739X. doi: https://doi.org/10.1016/j.future.2015.09.021. URL https://www.sciencedirect.com/science/article/pii/S0167739X15003015.

Xinyu Chen, Jiannan Tian, Ian Beaver, Cynthia Freeman, Yan Yan, Jianguo Wang, and Dingwen Tao. FCBench: Cross-domain benchmarking of lossless compression for floating-point data, 2024.

Yann Collet. Zstd, 2015. URL https://facebook.github.io/zstd.

James W. Cooley and John W. Tukey. An algorithm for the machine calculation of complex fourier series. *Mathematics of Computation*, 19(90):297–301, 1965. ISSN 00255718, 10886842. URL http://www.jstor.org/stable/2003354.

Hazem Elmeleegy, Ahmed K. Elmagarmid, Emmanuel Cecchet, Walid G. Aref, and Willy Zwaenepoel. Online piece-wise linear approximation of numerical streams with precision guarantees. *Proc. VLDB Endow.*, 2(1):145–156, 2009.

F. Gritzali and G. Papakonstantinou. A fast piecewise linear approximation algorithm. *Signal Processing*, 5(3):221–227, 1983.

Peeyush Gupta, Michael J. Carey, Sharad Mehrotra, and Roberto Yus. SmartBench: A benchmark for data management in smart spaces. *Proc. VLDB Endow.*, 13(11):1807–1820, 2020.

Udaiprakash I. Gupta, D. T. Lee, and Joseph Y.-T. Leung. Efficient algorithms for interval graphs and circular-arc graphs. *Networks*, 12(4):459–467, 1982.

S. Louis Hakimi and Edward F. Schmeichel. Fitting polygonal functions to a set of points in the plane. *CVGIP Graph. Model. Image Process.*, 53(2):132–136, 1991.

Søren Kejser Jensen, Torben Bach Pedersen, and Christian Thomsen. Modelardb: Modular model-based time series management with spark and cassandra. *Proc. VLDB Endow.*, 11(11):1688–1701, 2018.

Søren Kejser Jensen, Torben Bach Pedersen, and Christian Thomsen. Demonstration of ModelarDB: Model-based management of dimensional time series. In *SIGMOD*, pp. 1933–1936, 2019.

Panagiotis Karras and Nikos Mamoulis. Hierarchical synopses with optimal error guarantees. *ACM Trans. Database Syst.*, 33(3):18:1–18:53, 2008.

Eamonn J. Keogh, Kaushik Chakrabarti, Michael J. Pazzani, and Sharad Mehrotra. Dimensionality reduction for fast similarity search in large time series databases. *Knowl. Inf. Syst.*, 3(3):263–286, 2001a. doi: 10.1007/PL00011669. URL https://doi.org/10.1007/PL00011669.

Eamonn J. Keogh, Selina Chu, David M. Hart, and Michael J. Pazzani. An online algorithm for segmenting time series. In *Proc. IEEE International Conference on Data Mining*, pp. 289–296, 2001b.

Xenophon Kitsios, Panagiotis Liakos, Katia Papakonstantinopoulou, and Yannis Kotidis. Sim-piece: Highly accurate piecewise linear approximation through similar segment merging. *Proc. VLDB Endow.*, 16(8):1910–1922, 2023.

Xenophon Kitsios, Panagiotis Liakos, Katia Papakonstantinopoulou, and Yannis Kotidis. Flexible grouping of linear segments for highly accurate lossy compression of time series data. *VLDB J.*, 33(5):1569–1589, 2024.

Maximilian Kuschewski, David Sauerwein, Adnan Alhomssi, and Viktor Leis. BtrBlocks: Efficient columnar compression for data lakes. *Proc. ACM Manag. Data*, 1(2):118:1–118:26, 2023.

Iosif Lazaridis and Sharad Mehrotra. Capturing sensor-generated time series with quality guarantees. In *ICDE*, pp. 429–440, 2003.

Ruiyuan Li, Zechao Chen, Ruyun Lu, Xiaolong Xu, Guangchao Yang, Chao Chen, Jie Bao, and Yu Zheng. *Serf*: Streaming error-bounded floating-point compression. *Proc. ACM Manag. Data*, 3(3):216:1–216:27, 2025.

Panagiotis Liakos, Katia Papakonstantinopoulou, and Yannis Kotidis. Chimp: Efficient lossless floating point compression for time series databases. *Proc. VLDB Endow.*, 15(11):3058–3070, 2022.

Panagiotis Liakos, Katia Papakonstantinopoulou, Thijs Bruineman, Mark Raasveldt, and Yannis Kotidis. How to make your duck fly: Advanced floating point compression to the rescue. In *Proceedings 27th International Conference on Extending Database Technology, EDBT 2024, Paestum, Italy, March 25 - March 28*, pp. 826–829. OpenProceedings.org, 2024.

Ge Luo, Ke Yi, Siu-Wing Cheng, Zhenguo Li, Wei Fan, Cheng He, and Yadong Mu. Piecewise linear approximation of streaming time series data with max-error guarantees. In *ICDE*, pp. 173–184, 2015.

Joseph O'Rourke. An on-line algorithm for fitting straight lines between data ranges. *Commun. ACM*, 24(9):574–578, 1981.

Theodosios Pavlidis. Waveform segmentation through functional approximation. *IEEE Trans. Computers*, 22(7):689–697, 1973.

Tuomas Pelkonen, Scott Franklin, Paul Cavallaro, Qi Huang, Justin Meza, Justin Teller, and Kaushik Veeraraghavan. Gorilla: A fast, scalable, in-memory time series database. *Proc. VLDB Endow.*, 8(12):1816–1827, 2015.

Henry Stone. Approximation of curves by line segments. *Mathematics of Computation*, 15(73): 40–47, 1961.

Li Da Xu, Wu He, and Shancang Li. Internet of things in industries: A survey. *IEEE Trans. Ind. Informatics*, 10(4):2233–2243, 2014.

Yuanyuan Yao, Lu Chen, Ziquan Fang, Yunjun Gao, Christian S. Jensen, and Tianyi Li. *Camel:* efficient compression of floating-point time series. *Proc. ACM Manag. Data*, 2(6):227:1–227:26, 2024.

A APPENDIX

Table 2: Compression ratio comparison for $\epsilon = 5\%$ and $\epsilon = 10\%$ of the signal's range.

		5%						10.0%					
	CAMEL	SLIDE	MIXED	MIXPIECE	MINSEGMENTS	TAILORPIECEGD ($q=0$)	TAILORPIECEDP ($p=2^{-20}$)	SLIDE	MIXED	MIXPIECE	MINSEGMENTS	TAILORPIECEGD ($q=0$)	TAILORPIECEDP ($p=2^{-20}$)
Adiac	3.83	24.65	36.00	53.44	58.24	58.81	**63.25**	29.02	43.41	75.00	80.61	80.23	**83.98**
Beef	3.95	41.20	53.41	66.75	77.50	77.42	**85.91**	70.06	88.54	113.65	133.57	135.25	**147.93**
BirdChicken	3.81	40.35	56.34	59.60	71.20	70.77	**77.06**	55.65	78.77	84.45	109.74	107.86	**126.61**
Car	3.82	55.00	78.64	89.00	108.83	109.80	**125.27**	85.43	122.66	146.54	178.00	176.63	**214.53**
CinCECGTorso	4.03	248.45	349.04	352.11	419.07	432.90	**477.04**	413.22	523.56	558.27	669.46	713.65	**746.27**
DiatomSizeReduction	3.82	46.87	69.42	93.60	110.10	108.14	**122.19**	56.72	85.07	135.96	152.41	151.00	**164.54**
EthanolLevel	3.46	152.44	224.22	224.09	282.88	286.02	**348.43**	233.65	327.33	332.36	421.50	437.16	**528.40**
Fish	3.81	92.42	115.61	168.31	203.15	214.65	**222.10**	308.17	312.01	414.29	440.77	463.77	**517.46**
FreezerRegularTrain	3.70	63.23	67.68	131.30	148.42	148.89	**152.58**	91.66	95.56	238.59	233.78	244.28	**248.68**
Fungi	3.65	33.32	47.87	64.98	69.39	72.54	**80.50**	47.93	67.78	104.74	102.00	107.73	**121.49**
GunPoint	3.70	22.93	33.22	44.73	52.08	50.97	**58.20**	33.71	44.38	57.69	65.22	68.95	**74.01**
GunPointAgeSpan	2.84	30.12	37.88	54.95	63.39	64.24	**71.23**	57.72	67.48	100.93	120.45	125.54	**132.10**
GunPointMaleVersusFemale	2.99	30.63	38.30	55.97	64.47	65.36	**72.37**	59.24	72.16	103.80	123.56	128.09	**135.57**
GunPointOldVersusYoung	2.85	31.42	39.09	56.40	65.28	65.44	**73.03**	60.43	69.38	104.18	127.40	129.72	**138.17**
HandOutlines	3.90	180.02	269.91	293.15	377.18	374.71	**473.93**	212.77	280.90	292.72	423.73	444.20	**487.51**
Haptics	3.82	105.76	122.32	171.90	206.61	210.53	**223.84**	247.53	307.69	402.62	478.18	481.93	**510.86**
Herring	3.77	41.60	59.17	69.53	85.33	85.47	**96.29**	66.57	90.08	117.21	145.19	146.00	**166.02**
HouseTwenty	4.71	23.07	24.62	65.37	65.12	65.52	**65.61**	29.13	29.87	76.42	76.58	77.23	**78.34**
InlineSkate	3.81	226.50	306.28	304.18	373.66	378.79	**418.63**	386.85	536.19	519.82	616.33	638.98	**746.97**
LargeKitchenAppliances	4.23	104.06	121.80	195.79	205.66	211.42	**214.02**	162.34	182.15	314.22	324.68	332.23	**354.93**
Lightning2	3.90	80.00	100.17	141.95	154.08	159.54	**169.40**	185.95	226.03	313.00	330.27	358.71	**373.48**
Mallat	3.75	31.79	43.90	56.27	65.55	65.63	**72.44**	56.53	72.39	98.11	114.56	117.13	**129.09**
Meat	4.04	51.03	69.73	123.59	132.25	131.68	**144.03**	61.86	82.14	150.38	154.37	161.08	**172.45**
MixedShapesRegularTrain	3.84	67.32	94.30	104.41	123.80	124.15	**143.88**	95.60	128.95	149.25	188.19	188.28	**221.42**
NonInvasiveFetalECGThorax1	3.79	78.59	116.35	142.73	169.28	176.91	**194.46**	114.09	150.26	209.81	239.81	258.98	**286.33**
NonInvasiveFetalECGThorax2	3.79	75.99	113.19	139.25	163.03	171.27	**184.97**	115.08	146.31	209.15	235.71	253.49	**278.45**
PigAirwayPressure	3.93	199.20	287.36	296.52	390.24	391.39	**425.99**	284.09	416.67	442.97	536.19	569.80	**643.09**
PigArtPressure	3.65	38.66	52.77	66.51	80.92	82.14	**90.59**	75.47	92.29	129.01	140.40	161.65	**170.87**
PigCVP	3.73	48.08	60.42	66.81	82.35	80.89	**90.39**	118.69	133.33	159.05	201.26	197.53	**210.80**
Rock	3.92	357.14	465.12	466.74	519.48	539.81	**557.10**	719.42	847.46	911.16	1012.66	1010.10	**1084.01**
ShapesAll	3.82	42.03	58.31	70.65	84.87	84.46	**96.25**	61.26	84.14	105.08	133.38	131.73	**152.56**
SmallKitchenAppliances	4.21	38.39	45.45	93.09	93.20	95.03	**96.15**	50.02	59.56	113.99	114.81	120.59	**121.10**
StarLightCurves	3.81	170.79	234.74	231.68	287.36	293.79	**332.23**	236.97	343.05	344.38	428.95	456.36	**541.64**
Symbols	3.81	53.19	70.95	86.68	102.59	104.78	**117.23**	79.52	106.44	145.83	176.80	179.01	**198.91**
Trace	3.69	49.46	67.20	104.31	112.65	117.96	**123.77**	75.86	93.86	166.41	168.78	183.49	**190.48**
UMD	4.58	17.61	25.45	42.16	41.27	44.19	**45.37**	31.51	34.62	66.69	69.72	73.87	**76.49**
UWaveGestureLibraryX	3.83	50.26	66.38	83.02	98.79	101.37	**113.07**	107.99	120.85	169.24	209.42	212.99	**228.57**
UWaveGestureLibraryY	3.80	45.53	59.47	76.23	88.17	90.49	**99.96**	88.73	107.58	141.94	177.31	179.13	**192.91**
UWaveGestureLibraryZ	3.84	38.68	51.15	65.80	76.20	78.05	**86.26**	71.05	87.18	114.91	141.37	144.01	**157.26**
Wafer	3.74	25.40	26.56	63.87	66.05	66.81	**68.06**	100.81	118.27	198.12	194.03	215.69	**226.12**
Yoga	3.82	37.15	51.83	63.88	76.00	77.43	**86.59**	51.91	71.12	95.82	116.01	116.03	**134.00**
Average	3.80	77.81	105.16	126.86	149.16	151.95	**167.31**	133.91	169.45	212.87	246.52	255.61	**280.84**
Average (rest)	3.79	13.54	17.50	28.70	30.95	31.35	**32.99**	29.70	35.60	58.24	63.22	64.99	**68.19**
Average (all)	3.79	38.40	51.41	66.67	76.67	78.00	**84.94**	70.00	87.37	118.05	134.12	138.72	**150.44**

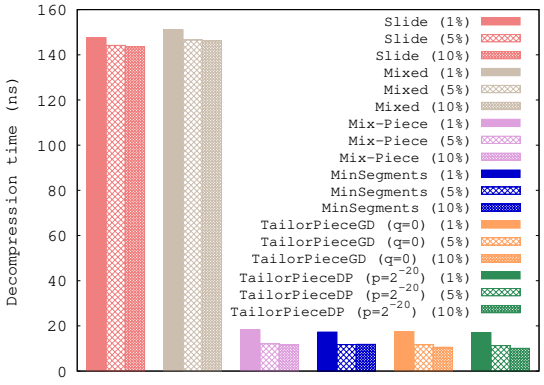

Figure 12: Decompression time per record.

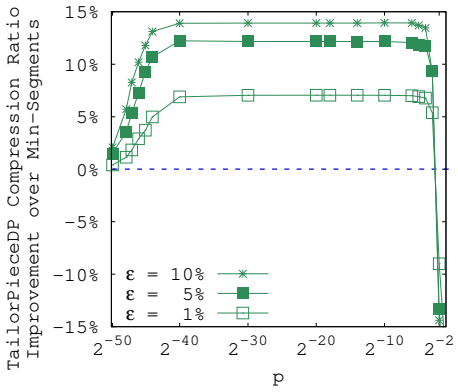

Figure 13: Average improvement vs. p.